

# INVESTIGATION OF A MODEL FOR CONTROLLING DISSOLVED OXYGEN CONCENTRATION IN CRAB PONDS

Ho Ngoc Ha<sup>1\*</sup>, Minh Hoa Nguyen<sup>2</sup>, Duong Van Cham<sup>3</sup>

**Abstract** – *Nowadays, aquaculture, especially crab farming, is given special attention to development. However, the control of dissolved oxygen concentration in crab ponds has not been widely studied. Therefore, the purpose of the project is to study a model to control the dissolved oxygen concentration in water in a ratio appropriate to the weather and climate conditions in Tra Vinh Province, Vietnam. The study uses data collection and processing of actual data from the crab farming environment in the pond to find the most suitable control model, thereby adjusting the dissolved oxygen concentration to suit the atmospheric conditions of the local post. Data is collected through sensors installed directly on the pond. Then it is processed with Matlab Simulink software to check the effectiveness of the models. The results of this study show that the artificial neural network model is the most suitable model for applying dissolved oxygen concentration control. Research results can be used to improve dissolved oxygen concentration adjustment devices, increasing the productivity, quality, and production efficiency of the aquaculture industry.*

**Keywords:** *artificial neural network, crab ponds, dissolved oxygen.*

## I. INTRODUCTION

Dissolved oxygen (DO) concentration, an important factor for the health and productivity of aquatic organisms, has not received adequate attention in Vietnam, especially in crab farming systems. Effective DO control is essential

to maintain optimal water quality and ensure sustainable aquaculture practices.

The research highlighted that pond farming involves open water areas where the distribution of dissolved oxygen is inherently three-dimensional. Traditional one-dimensional predictions at a single monitoring point fail to capture the actual spatial variation of dissolved oxygen within the pond. Initially, environmental factors influencing dissolved oxygen distribution were collected, and an attention-gated recurrent unit (GRU) model was developed to predict dissolved oxygen at a central monitoring point. Subsequently, a three-dimensional coordinate system was established centered on these monitoring points, employing the optimized gradient boost regression tree (GBRT) and random search (RS) algorithms to predict dissolved oxygen levels at any location within the pond. Experimental results demonstrated that the Attention-GRU-GBRT method could accurately predict dissolved oxygen in the three-dimensional spaces of ponds [1].

Xinhui et al. [2] utilized a round-robin experiment to explore the aeration gap of DO at varying air flow rates. The study identified gas flow rate and DO content as the main variables. In this work, a radius basis function (RBF) neural network proportional-integral-derivative (PID) controller, optimized by a differential evolution (DE) algorithm (DE-RBF-PID), is proposed. This controller includes two significant optimizations: firstly, the improved DE algorithm determines the optimal initial PID parameters; secondly, the RBF neural network's learning ability allows for online adjustment of these parameters, effectively eliminating overshoot and improving adaptability. Simulations on a typical nonlinear DO control system confirm the superiority of the DE-RBF-PID controller over traditional PID and RBF-

<sup>1,2</sup>Tra Vinh University, Vietnam

<sup>3</sup>Duyen Hai Thermal Power Company, Vietnam

\*Corresponding author: [haha@tvu.edu.vn](mailto:haha@tvu.edu.vn)

Received date: 03<sup>rd</sup> July 2024; Revised date: 06<sup>th</sup> November 2024; Accepted date: 08<sup>th</sup> November 2024

PID controllers, making it a promising solution for precise tracking control of DO in complex aquaculture environments.

This study outlines the research methodology, emphasizing data collection via smart sensor devices directly installed in the pond environment. Subsequently, advanced algorithmic models, including the artificial neural network (ANN) and the ARMAX linear regression model, are implemented using Matlab/Simulink for data analysis and interpretation. From there, the results of the models were analyzed and compared to find the most suitable control model to adjust dissolved oxygen concentration in accordance with local climatic conditions.

## II. LITERATURE REVIEW

### A. Dynamic model design

Aquatic macrophytes are commonly cultivated by farmers to sustain DO levels in crab ponds, serving as the primary source of photosynthetic oxygen. This study also incorporates the influence of phytoplankton and protists on DO within the scope of aquatic macrophytes. An air diffusion aeration system was selected as the focus of the research due to its superior oxygen transfer capabilities. Crab ponds are considered a closed ecosystem with no water exchange with the external environment. For modeling purposes, the biomass of aquatic macrophytes was quantified in terms of dry weight ( $gm^{-3}$ ), while the organic matter content was expressed as  $mmolm^{-3}$ . The structural framework of the DO dynamic model, accounting for both physical and biochemical factors affecting oxygen flux, is illustrated in Figure 1.

The dynamics and equilibrium of DO are governed by the conditions of oxygen sources and sinks. To characterize the temporal behavior of DO, all relevant sources and sinks were incorporated to formulate a conservation equation, as presented in Equation (1).

$$\frac{dDO}{dt} = P + Rear + Aer + Rmac - Min - Rcrab \quad (1)$$

Where: *Rear*: water surface reaeration; *Aer*: oxygen transfer rate of mechanical aeration; *P*: the

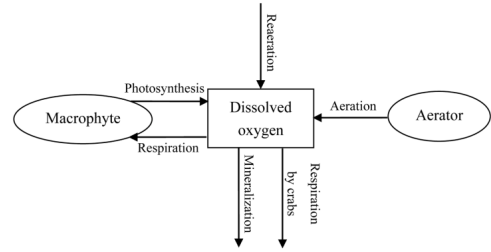


Fig. 1: The structure of a DO model in a crab pond

source terms including photosynthesis of aquatic macrophyte;  $R_{mac}$ : The sink terms of DO contain respiration by aquatic macrophyte;  $R_{crab}$ : respiration by crabs;  $Min$ : mineralization of organic matter.

### B. Mathematical procedures and formulas

#### Photosynthesis of aquatic macrophyte

Photosynthesis is a process where chlorophyll captures light energy and transforms carbon dioxide and water into energy-rich organic compounds, releasing oxygen in the process. Thus, the photosynthetic rate is generally considered proportional to the biomass of aquatic macrophytes. The primary production of these plants is influenced by three key external factors: solar radiation, temperature, and nutrient availability [3]. Mandal et al. [4] take photoinhibition into account, and the formula for oxygen production by aquatic plants through photosynthesis is presented in Equation (2).

$$P = P_{max} \times \left( \frac{I}{I_{opt}} \right) e^{\left( 1 - \left( \frac{I}{I_{opt}} \right) \right)} \times B \quad (2)$$

Where:  $P_{max}$ : daily maximum oxygen production rate influenced by water temperature;  $I_{opt}$ : optimum solar radiation for macrophyte;  $B$ : macrophyte biomass;  $I$ : the water surface light intensity.

Plus et al. [5] stated that the maximum oxygen production rate ( $P_{max}$ ) is influenced by water temperature ( $T$ ). To estimate  $P_{max}$  for ten aquatic

plant species, both linear and exponential regression models were applied. In this research, exponential regression was used to illustrate the relationship between  $P_{max}$  and  $T$ , with the relevant calculation provided in Equation (3).

$$P_{max} = a \times e^{bT} \quad (3)$$

Where:  $b$ : temperature coefficient;  $a$ : regression coefficient.

Their exact value will be obtained by parameter optimization.

### Respiration of aquatic macrophytes

Respiration is a vital metabolic process where organic matter breaks down into carbon dioxide and water, releasing energy necessary for plant growth. Ondok et al. [6] noted that the respiration of aquatic macrophytes is influenced by temperature, with respiration rates increasing as water temperature rises. Exponential regression was applied in this study to model the changes in respiration rates based on temperature. Equations (4) and (5) describe the respiration process of aquatic plants.

$$R = resp \times B \quad (4)$$

$$Resp = m \times e^{nT} \quad (5)$$

Where:  $m$ : regression coefficient;  $resp$ : limitation function of water temperature;  $n$ : temperature coefficient

### Surface regeneration

Haider et al. [7] explained that the reaction involves a diffusion process between DO in the water and atmospheric oxygen. The oxygen exchange at the water surface is controlled by the gradient between the DO concentration and the oxygen saturation level in the water. The formula for calculating water surface regeneration is presented in Equation (6).

$$R_{ear} = K_e (DO_{sat} - DO) \quad (6)$$

Where:  $DO_{sat}$ : saturation content of DO;  $K_e$ : the reaeration coefficient.

$$DO_{sat} = 14.625 - 0.41022T + 7.99 \times 10^{-3}T^2 - 7.7774 \times 10^{-5}T^3 \quad (7)$$

$DO_{sat}$  is calculated with temperature in Equation (7). The response coefficient is influenced by wind speed and temperature. As stated by Antonopoulos et al. [8],  $K_e$  can be calculated using Equations (8) and (9).

$$K_{e20} = \begin{cases} 0.2 W & , W \leq 3.5 \text{ m/s} \\ 0.057 W^2 & , W > 3.5 \text{ m/s} \end{cases} \quad (8)$$

$$K_e = K_{e20} \cdot \theta_r^{T-20} \quad (9)$$

Where:  $\theta_r$ : reaeration temperature coefficient at 1.024;  $W$ : wind speed;  $K_{e20}$ : reaeration coefficient at 20°C.

### Mechanical aeration

Diffusion aeration systems utilize a high-volume air blower to deliver air to diffusers placed in the water. Various types of diffusers are used in crab farming, including porous ceramic tubes, perforated rubber tubes, and perforated plastic tubes [9]. The rate of oxygen transfer is influenced by the gradient between the DO concentration and oxygen saturation in the water, as well as the water temperature. The actual oxygen transfer rate for an aeration diffuser system operating in a fish pond can be calculated using Equation (10).

$$A_{er} = S_{OTR} \times \frac{DO_{sat} - DO}{9.09} \times \theta_a^{T-20} \times \frac{24}{\text{volume}} \times \alpha \times s \quad (10)$$

Where:  $\theta_a$ : aeration temperature coefficient;  $S_{OTR}$ : the oxygen transfer rate under standard conditions (20°C);  $volume$ : the volume of the crab pond;  $\alpha$  environmental correction constant to correct the error between a crab pond and the test water;  $s$ : the working status (on or off) of the aerator.

### Mineralize

Heterotrophic microorganisms break down particulate organic matter into inorganic matter through mineralization, which can then be utilized for the growth of aquatic organisms. This

process is crucial for material cycling within the ecosystem [10]. Chappelle et al. [11] noted that in the water column, mineralization is temperature-dependent. The formula for calculating mineralization is provided in Equation (11).

$$M_{in} = min_0 \times e^{kT} \times O_{om} \times C_{om} \quad (11)$$

Where:  $kT$ : temperature coefficient of the biochemical reactions;  $min_0$ : the rate of mineralization at  $0^\circ C$ ;  $O_{om}$ :  $O_2$  consumed per mmole of organic matter mineralized;  $C_{om}$ : the content of organic matter.

### Crab respiration

As a key species in aquaculture, crabs require oxygen and energy for locomotion, growth, and digestion. The assimilation process in crabs relies on oxygen consumption for metabolic activities, resulting in a reduction of DO levels. Zou et al. [12] investigated the effects of body mass and temperature on the respiration rate of crabs. Comparative experiments were conducted using *Eriocheir sinensis* of various sizes, as outlined in Equation (12) was used in this work to calculate the respiratory rate.

$$R_{crab} = \frac{A}{1 + e^{(2.351 - 0.138T)}} \times M^\beta \quad (12)$$

Where:  $R_{crab}$ : Crab respiration;  $M$ : crab mass ( $g \cdot m^{-3}$ );  $A$ : the limitation of crab respiration;  $\beta$  a negative constant of crab mass coefficient.

### C. Distributed dissolved oxygen at different depths

The one-dimensional vertical transport of DO in crab ponds according to Solomon et al. [13] is described by the diffusion equation in the form of Equation (13).

$$\frac{\partial DO}{\partial t} = D \frac{\partial^2 DO}{\partial z^2} + S \quad (13)$$

Where:  $D$ : the diffusion coefficient ( $m^2 \cdot day^{-1}$ );  $z$ : the pond depth;  $S$ : the term of all DO sources and sinks acting in each layer.

In pond environments, the diffusion coefficient of oxygen ( $D$ ) is typically modeled based on the

horizontal area and the steady-state frequency associated with water density [14]. However, since crab ponds are much shallower than lakes, the vertical stratification affecting aquaculture waters is less significant. As a result, in this study, the diffusion coefficient is assumed to be constant across both depth and time. Since water absorbs portions of the light spectrum, irradiance decreases with depth. To account for the reduction of solar radiation and its effect on the vertical distribution of DO, the formula representing the variation of solar radiation with depth is applied, as shown in Equation (14).

$$I_z = I \cdot e^{(-EC \cdot z)} \quad (14)$$

Where:  $I$ : solar radiation at water surface;  $I_z$ : solar radiation at depth  $z$ ;  $EC$ : the extinction coefficient of water.

The ordinary differential Equation (1) is solved using the four-step Runge-Kutta method with a time step of 10 minutes. The detailed calculation steps of this method are provided by Hussain et al. [15]. The partial differential Equation (13) is solved using the semi-implicit Crank-Nicolson method. Unlike explicit and implicit finite difference methods, which impose restrictions on the diffusion coefficient, time step size, and layer thickness, the Crank-Nicolson method offers a stable numerical solution to the diffusion equation without these limitations. After applying the Crank-Nicolson discretization scheme, Equation (13) is reformulated as Equation (15).

$$rDP_{i+1,j+1} = -rDP_{i-1,j+1} + (2 + 2rD)P_{i,j+1} - rDP_{i-1,j} - (2 - 2rD)P_{i,j} - rDP_{i+1,j} - \frac{1}{2}\Delta t(S_{i,j} + S_{i,j+1}) \quad (15)$$

Where:  $P_i$ ,  $P_j$  represents the content of DO in space  $z$  ( $z = i\Delta t$ ) and time  $t$  ( $t = j\Delta t$ ) and  $r = \frac{\Delta t}{(\Delta x)^2}$ ). Finally, a system of linear algebraic equations, with a triangular matrix, is obtained in

the form of Equation (16).

$$\begin{bmatrix} 2+2rD & -rD & 0 & \dots & 0 & 0 & 0 \\ 0 & -rD & 2+2rD & \dots & 0 & 0 & 0 \\ \vdots & \vdots & \vdots & \ddots & \vdots & \vdots & \vdots \\ 0 & 0 & 0 & \dots & 2-2rD & rD & 0 \\ 0 & 0 & 0 & \dots & 0 & rD & 2-2rD \end{bmatrix} \begin{bmatrix} P_{1,j+1} \\ P_{2,j+1} \\ \vdots \\ P_{N-3,j+1} \\ P_{N-2,j+1} \end{bmatrix} \\ = \begin{bmatrix} 2rDP_{0,j} + (2-2rD)P_{1,j} + rDP_{2,j} \\ 2rDP_{1,j} + (2-2rD)P_{2,j} + rDP_{3,j} \\ \vdots \\ 2rDP_{N-4,j} + (2-2rD)P_{N-3,j} + rDP_{N-2,j} \\ 2rDP_{N-3,j} + (2-2rD)P_{N-2,j} + rDP_{N-1,j} \end{bmatrix} + \begin{bmatrix} \frac{1}{2}t(S_{1,j} + S_{1,j+1}) \\ \frac{1}{2}t(S_{2,j} + S_{2,j+1}) \\ \vdots \\ \frac{1}{2}t(S_{N-3,j} + S_{N-3,j+1}) \\ \frac{1}{2}t(S_{N-2,j} + S_{N-2,j+1}) \end{bmatrix} \quad (16)$$

The above system of linear equations is solved by the Thomas algorithm.

#### D. Model analysis, validation, and sensitivity

To ensure that the model output aligns with real-world conditions, calibration of the model is essential. Since the photosynthesis and respiration rates of aquatic macrophytes vary, and the oxygen transfer rates of aerators differ across various water environments, it is necessary to adjust the parameters involved in these processes. Parameter optimization is achieved using the Levenberg-Marquardt algorithm. The computational procedures for the Levenberg-Marquardt algorithm are detailed in Ampazis et al. [16]. To evaluate the model's performance, test data not used during calibration are employed for validation. The mean absolute percentage error (MAPE) is used as a metric for model performance, with the calculation formulas provided in Equation (17).

$$MAPE = \frac{100}{N} \times \sum_{i=1}^N \left| \frac{y_i - \bar{y}_i}{y_i} \right| \quad (17)$$

Where:  $y_i$ : the measurement;  $\bar{y}_i$ : the model prediction;  $N$ : the number of samples

Sensitivity analysis was used to measure the influence of model parameters on DO changes. The sensitivity analysis formula is a list like Equation (18).

$$Sensitivity = \frac{100}{r} \times \frac{1}{n} \times \sum_{i=1}^n \frac{|v_i - \bar{v}_i|}{v_i} \quad (18)$$

Where:  $n$ : the sample number simulated;  $r$ : the variation range of parameters (+ 10% or - 10%);  $v_i$ : the new variable value of DO;  $\bar{v}_i$ : the original value simulated.

### III. INVESTIGATION DESIGN

#### A. Survey model structure

The control cabinet includes devices: Buck circuit, power supply relay module, ESP 8266 module, TTL to RS485 module used to switch devices and transmit data to computers or other smart devices, DO sensor, pH measuring sensor, temperature and humidity sensor, rain flow sensor, salinity sensor, and wind speed sensor. The system's power sources include a 220 V AC grid connection and a 12 V DC solar battery (30 W). A power supply switch allows toggling between grid power and solar power. A buck converter circuit steps down the 12 V DC to 5 V DC, supplying power to the ESP8266 module and the USB 4G modem, both of which require a minimum current of 1,200 mA. A relay module controls the 12 V power supply to the TTL-to-RS485 module. The ESP8266 module reads data from sensors through the TTL-to-RS485 module, then sends the data to a website for storage, and connects to a Wi-Fi signal provided by the 4G USB modem. It reads sensor data every 15 minutes, updates the website with new data, and repeats the cycle continuously. The TTL-to-RS485 module reads sensor signals, converts them, and sends them to the ESP8266 module. The TTL to RS485 conversion circuit is designed with the UART communication standard, to convert communication from the RS485 standard to the TTL standard and vice versa (suitable for all types of microcontrollers and embedded computers). Sensors that collect pond environmental parameters (oxygen concentration sensor, water temperature sensor, pH sensor, humidity sensor, air temperature precipitation sensor, and wind speed sensor). Each type of sensor was set up with a different ID due to the ModbusPoll application. The signals from the sensors are connected and transmitted through two wires RS485A+ and RS485B-. The measurement signal from the sensor was saved in

the corresponding registers, the actual value was read and decoded by the ESP 8266, then the data was sent to the website every 15 minutes.

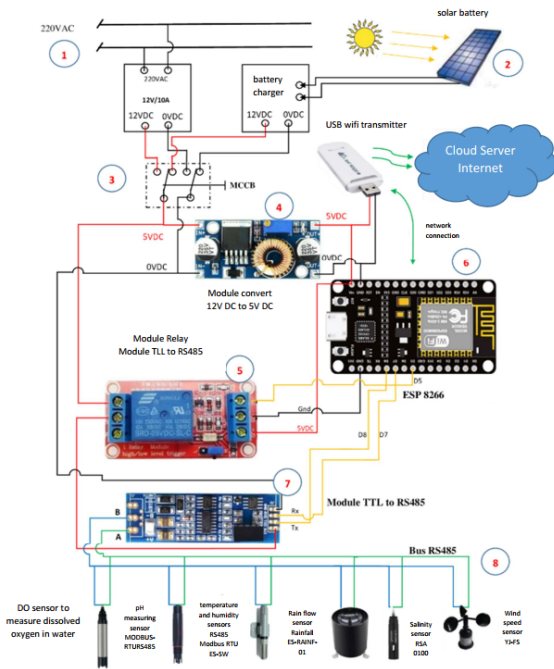


Fig. 2: Device structure used in the model

**B. Realistic model**



Fig. 3: Crab pond and actual model used for the research

The system design is used in crab farming ponds in Duyen Hai District, Tra Vinh Province, with a total crab farming area of 1,200 m<sup>2</sup>, with an output of 850 crabs, the age of crabs was about a month with an annual output of 300 kg. The crab pond is a rectangle with length, width, and depth dimensions of 100 m, 12 m, and 1.5 m, respectively. The selection of experimental crabs in pond water took place in October 2022. The age of the crabs was about 1.5 months and the crabs were in the development stage. The pH of the water ranges from 7.71 to 7.98 and the water temperature ranges from 28°C to 30.31°C. Data collected from 13<sup>th</sup> to 17<sup>th</sup> October 2022 includes: data on DO content, temperature measured directly by a sensor placed in the middle of the pond and measured every 15 minutes, and wind speed estimated according to the results and measured by the local meteorological management agency.

**C. Algorithm used in simulation**

The data collected from sensors in two time frames, 24 hours and 96 hours, is used in the article. Simulations are then conducted, incorporating three models: physical models, neural networks models, and ARMAX models.

In the physical models, the mathematical equations presented in Section II are applied and then compared with the simulation results obtained from the collected data.

In the artificial neural network model, simulations are conducted using three algorithms: Levenberg-Marquardt, Bayesian regularization, and scaled conjugate gradient. Each algorithm simulates networks with 10, 15, 20, 25, and 30 hidden neurons.

Figure 5 depicts an artificial neural network model on Matlab Simulink with DOinputseries as input data from pH sensors, temperature sensors, salinity sensors located at crab ponds, and DOrealoutseries taking data from DO sensor located at the crab pond.

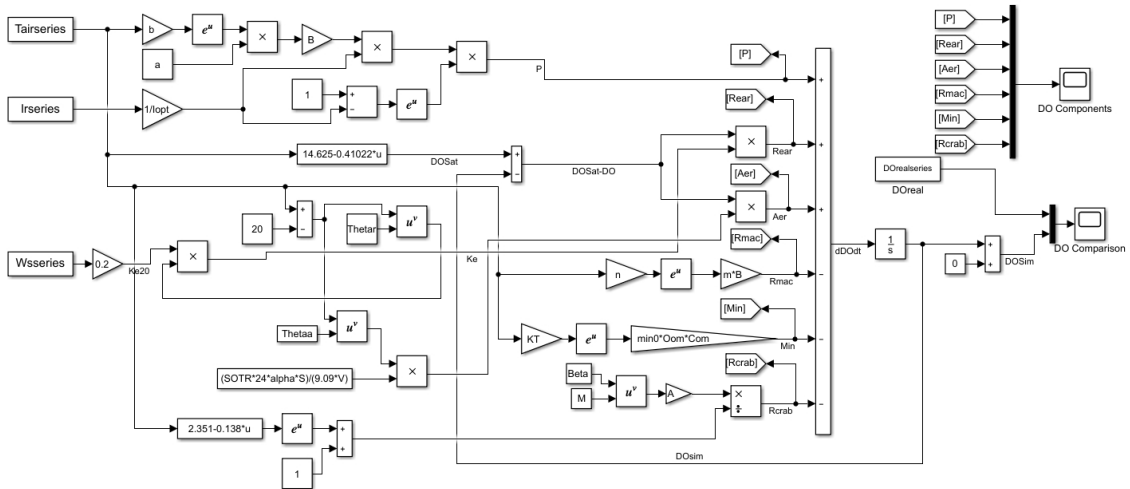


Fig. 4: The physical model in Matlab Simulink

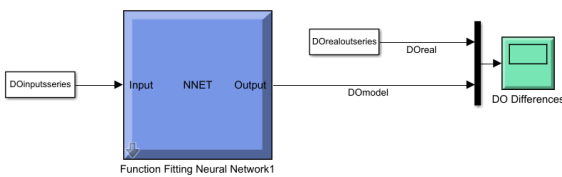


Fig. 5: The artificial neural network model in Matlab Simulink

In the regression network model, three algorithms including Levenberg Marquardt, Bayesian regularization, and scaled conjugate gradient are simulated.

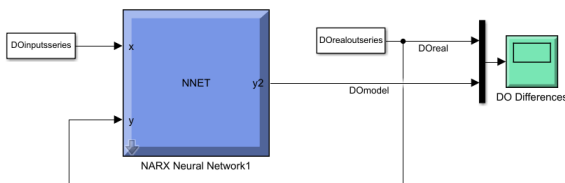


Fig. 6: The regression network model in Matlab Simulink

Figure 6 is a regression network model on

Matlab Simulink with DOinputseries as input data from pH sensors, temperature sensors, and salinity sensors located at crab ponds, DOrealoutseries taking data from DO sensor located at the crab pond, and linear regression data is DOrealoutseries.

D. Determine parameters

Table 1 presents the simulation parameters for algorithms in Matlab Simulink as presented in Equation (1).

IV. RESULTS AND DISCUSSION

A. Simulation based on the physical models in Matlab Simulink

Applying Equation (1) in the simulation using Matlab Simulink produces the dashed line in Figure 7, while the actual data collected from the experimental crab pond produces the solid line in Figure 7.

The physical model used mathematical equations to simulate DO dynamics. However, as shown in Figure 7, the theoretical model’s predictions (dashed line) diverged significantly from the actual data (solid line). This inconsistency aligns with the limitations identified by Xinkai et al. [1], where traditional one-dimensional models could

Table 1: Controller parameters

Symbol	Value	Describe
T	real-time	water temperature
I	real-time	solar radiation
W	real-time	wind speed
B	100	macrophyte biomass
$C_{om}$	3	the content of organic matter
s	0 or 1	working status of the aerator
a	0.1100	regression coefficient
b	0.0760	temperature coefficient of photosynthesis
$I_{opt}$	300	optimum solar radiation for macrophyte
m	0.0096	regression coefficient
n	0.0400	temperature coefficient of macrophyte
$\theta_r$	1.0240	reaeration temperature coefficient
$S_{OTR}$	32	Standard oxygen transfer rate
$\theta_a$	1.0240	aeration temperature coefficient
V	1200	volume of pond water
$\alpha$	0.7	environmental correction constant
M	850	crab mass
$min_0$	0.2000	the rate of mineralization at 0°C
$k_T$	0.0630	temperature coefficient of mineralization
$O_{om}$	0.2120	O <sub>2</sub> consumed per mmol N mineralized
A	0.0300	the limitation of crab respiration
$\beta$	-0.5000	crab mass coefficient

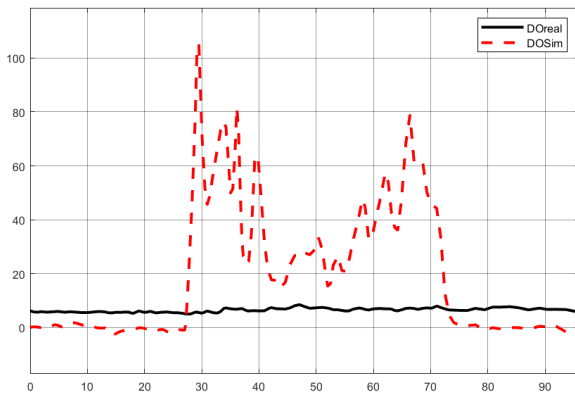


Fig. 7: Simulation results from the physical models

not capture the three-dimensional variations in DO levels accurately. Consequently, while the physical model demonstrated certain expected trends, its low correlation with real conditions in crab ponds suggests that physical models alone may not suffice for DO control in dynamic aquaculture environments.

*B. Simulation based on the artificial neural networks model in Matlab Simulink*

Figure 8 describes the simulation result from the neural network in 24-hour from three algorithms, Levenberg Marquardt, Bayesian regularization, and scaled conjugate gradient at 20 hidden neurons and 25 hidden neurons. The three first figures (Figure 8a, Figure 8b, Figure 8c) simulate the result from the Bayesian regularization algorithm, Levenberg-Marquardt algorithm, and scaled conjugate gradient algorithm at 20 hidden neurons, respectively. Then, the simulation results from the three algorithms at 25 hidden neurons are presented in Figure 8d, Figure 8e, Figure 8f. The solid line represents the actual 24-hour dissolved oxygen concentration and the dotted line represents the dissolved oxygen level when applying the artificial neural model. The above six results in the scaled conjugate gradient algorithm at 20 hidden neurons (Figure 8c) were compared for the best results.

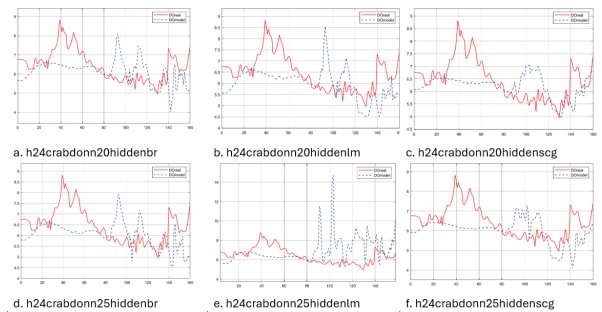


Fig. 8: Simulation results from the 24-hour simulated artificial neural network model

Figure 9 is the simulation result from the neural network in 96-hour from three algorithms, including Levenberg Marquardt, Bayesian regularization, and scaled conjugate gradient at 25

hidden neurons and 30 hidden neurons, detailed in Figure 9a, Figure 9b, Figure 9c, Figure 9d, Figure 9e, Figure 9f, respectively. The above six results in the scaled conjugate gradient algorithm at 30 hidden neurons were compared for the best results.

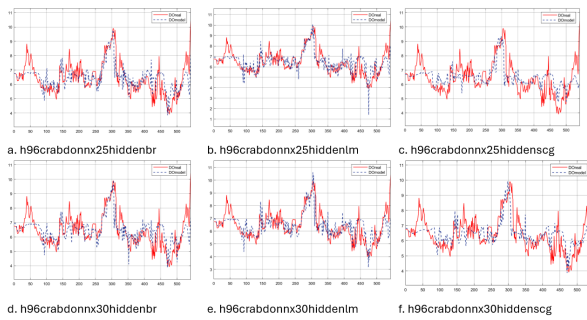


Fig. 9: Simulation results from the 96-hour simulated artificial neural network model

The artificial neural network model was evaluated across three algorithms: Bayesian regularization, Levenberg-Marquardt, and scaled conjugate gradient, with simulations conducted for both 24-hour and 96-hour intervals. The scaled conjugate gradient algorithm at 20 and 30 hidden neurons produced the most accurate results, closely aligning with actual DO levels (Figures 8c and 9f). This finding is consistent with previous research by Xinhui et al. [2], who found that adaptive models, particularly those incorporating neural network techniques, outperformed static physical models due to their flexibility in adjusting to real-time environmental changes.

### C. Simulation based on the regression network models in Matlab Simulink

The simulation results from the regression network models in Matlab Simulink over a 24-hour period are presented in Figure 10. Figure 10a displays the simulation results obtained using the Bayesian regularization algorithm with 10 hidden neurons. Figure 10b shows the simulation results from the Levenberg-Marquardt algorithm, also with 10 hidden neurons. Meanwhile, Figure 10c presents the simulation results from the

scaled conjugate gradient algorithm, again with 10 hidden neurons.

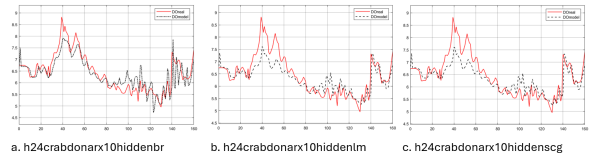


Fig. 10: Simulation results from the 24-hour simulated regression model

When simulating the system under a 24-hour regression model, the solid line represents the actual 24-hour dissolved oxygen concentration and the dotted line represents the dissolved oxygen level when applying the regression model. Simulation results from the regression model are quite good in the short term. However, when there are long-term changes, the results diminish.

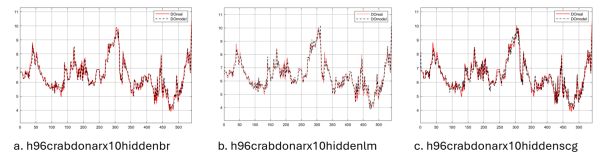


Fig. 11: Simulation results from the 96 hours simulated regression model

Figure 11 is the simulation result from the simulated regression model for 96 hours, the solid line represents the actual dissolved oxygen level, and the dotted line represents the dissolved oxygen level when applying the regression model. Simulation results from the regression model simulated for 96 hours when both curves are almost the same. From there, this model is quite accurate compared to reality.

Regression models, while more straightforward, showed promising results in short-term simulations (24 hours, Figure 10) but exhibited reduced accuracy in longer-term scenarios (96 hours, Figure 11). This aligns with Xinhui et al.'s findings [2], where short-term predictive models achieved high accuracy but struggled to adapt over extended periods without significant recalibration. Despite these limitations, the regression

model's effectiveness in short-term DO control suggests its potential for specific applications, such as short-term monitoring and rapid response in aquaculture systems.

From the simulation results presented above, for physical models that are not accurate to reality, it is necessary to find an optimal solution to adjust these parameters, such as genetic algorithm, swarm algorithm forums, artificial neural networks model, and regression network models that have a close connection to reality. However, the control devices in the regression network models are quite complex and expensive. Therefore, flexibly applying different control algorithms depending on actual conditions in aquaculture will help increase production efficiency and save energy.

## V. CONCLUSION

Equipment, including smart sensors such as dissolved oxygen sensors, temperature sensors, and pH sensors, was developed to collect data from crab ponds in Duyen Hai District, Tra Vinh Province, Vietnam. Data were gathered under varying conditions and at different times. Subsequently, Matlab Simulink software was employed to process the data using three models: physical models, artificial neural network models, and regression network models. Analysis of the simulation results indicates that the artificial neural network model is the most suitable for controlling dissolved oxygen concentration in practical applications, according to this study. These research findings can contribute to enhancing devices for adjusting dissolved oxygen concentration in crab ponds, helping crab farming households improve aquaculture productivity, quality, and production efficiency.

## REFERENCES

- [1] Xinkai C, Ni R, Ganglu T, Yuxing F, Qingling D. A three-dimensional prediction method of dissolved oxygen in pond culture based on Attention-GRU-GBRT. *Computers and Electronics in Agriculture*. 2021;181: 105955. <https://doi.org/10.1016/j.compag.2020.105955>.
- [2] Xinhui Z, Jianping W, Lin H, Daoliang L, Qingling D. Modelling and controlling dissolved oxygen in re-circulating aquaculture systems based on mechanism analysis and an adaptive PID controller. *Computers and Electronics in Agriculture*. 2022;192: 114–124. <https://doi.org/10.1016/j.compag.2021.106583>.
- [3] Stefan HG, Fang X. Dissolved oxygen model for regional lake analysis. *Ecological Modelling*. 1994;71(1): 37–68. [https://doi.org/10.1016/0304-3800\(94\)90075-2](https://doi.org/10.1016/0304-3800(94)90075-2).
- [4] Mandal S, Debnath M, Ray S, Ghosh PB, Roy M, Ray S. Dynamic modelling of dissolved oxygen in the creeks of Sagar island, Hooghly–Matla estuarine system, West Bengal, India. *Applied Mathematical Modelling*. 2012;36(12): 5952–5963. <https://doi.org/10.1016/j.apm.2011.10.013>.
- [5] Plus M, Chapelle A, Lazure P, Auby I, Levavasseur G, Verlaque M, et al. Modelling of oxygen and nitrogen cycling as a function of macrophyte community in the Thau lagoon. *Continental Shelf Research*. 2003;23(17): 1877–1898. <https://doi.org/10.1016/j.csr.2003.03.001>.
- [6] Ondok JP, Pokorny J, Kvet J. Model of diurnal changes in oxygen, carbon dioxide and bicarbonate content in a stand of *Elodea canadensis* Michx. *Aquatic Botany*. 1984;19(3): 293–305. [https://doi.org/10.1016/0304-3770\(84\)90045-7](https://doi.org/10.1016/0304-3770(84)90045-7).
- [7] Haider H, Ali W, Haydar S. Evaluation of various relationships of reaeration rate coefficient for modeling dissolved oxygen in a river with extreme flow variations in Pakistan. *Hydrological Processes*. 2013;27(26): 3949–3963. <https://doi.org/10.1002/hyp.9528>.
- [8] Antonopoulos VZ, Gianniou SK. Simulation of water temperature and dissolved oxygen distribution in Lake Vegoritis, Greece. *Ecological Modelling*. 2003;160(1): 39–53. [https://doi.org/10.1016/S0304-3800\(02\)00286-7](https://doi.org/10.1016/S0304-3800(02)00286-7).
- [9] Boyd CE. Pond water aeration systems. *Aquacultural Engineering*. 1998;18(1): 9–40. [https://doi.org/10.1016/S0144-8609\(98\)00019-3](https://doi.org/10.1016/S0144-8609(98)00019-3).
- [10] Matson PA, Vitousek PM. Nitrogen mineralization and nitrification potentials following clearcutting in the Hoosier National Forest, Indiana. *Forest Science*. 1981;27(4): 781–791. <https://doi.org/10.1093/forestscience/27.4.781>.
- [11] Chapelle A, Menesguen A, Deslouspaoli J, Souchu P, Mazouni N, Vaquer A, et al. Modelling nitrogen, primary production and oxygen in a Mediterranean lagoon. Impact of oyster farming and inputs from the watershed. *Ecological Modelling*. 2000;127(2): 161–181. [https://doi.org/10.1016/S0304-3800\(99\)00206-9](https://doi.org/10.1016/S0304-3800(99)00206-9).
- [12] Zou E, Du N, Lai W. The effects of mass temperature and thermal acclimation on the respiration rate of the Chinese freshwater crab *Eriocheir sinensis* (Crustacea: Decapoda). *Zoological Research*. 1995;16(1):

- 49–58.
- [13] Salomone MD, Herb W, Mohseni O, Stefan HG. *MCPLANT: A simulation model of dissolved oxygen production by aquatic macrophytes*. Project report. Minnesota, United States: University Digital Conservancy; 2000.
- [14] Hondzo M, Stefan HG. Lake water temperature simulation model. *Journal of Hydraulic Engineering*. 1993;119(11): 1251–1273. [https://doi.org/10.1061/\(ASCE\)0733-9429\(1993\)119:11\(1251\)](https://doi.org/10.1061/(ASCE)0733-9429(1993)119:11(1251)).
- [15] Hussain KA, Ismail F, Senu N, Rabiei F. Optimized fourth-order runge-kutta method for solving oscillatory problems. *AIP Conference Proceedings*. 2016;1739(1): 20–32. <https://doi.org/10.1063/1.4952512>.
- [16] Ampazis N, Perantonis SJ. Levenberg-Marquardt algorithm with adaptive momentum for the efficient training of feedforward networks. In: *Proceedings of the IEEE-INNS-ENNS International Joint Conference on Neural Networks. IJCNN 2000O. Neural Computing: New Challenges and Perspectives for the New Millennium*. 27<sup>th</sup> July 2000; Como, Italy. IEEE; 2000. <https://doi.org/10.1109/IJCNN.2000.857825>.

